The loss of *DLG2* isoform 7/8, but not isoform 2, is critical in advanced staged neuroblastoma

Simon Keane
University of Skovde: Hogskolan i Skovde
Tommy Martinsson
University of Gothenburg: Goteborgs Universitet
Per Kogner
Karolinska Institute: Karolinska Institutet
Katarina Ejeskar (katarina.ejeskar@his.se)
Hogskolan i Skovde

Research

Keywords: Neuroblastoma, DLG2, LIN7A, L27, Isoform

Posted Date: October 1st, 2020

DOI: https://doi.org/10.21203/rs.3.rs-83298/v1

Version of Record: A version of this preprint was published at Cancer Cell International on March 16th, 2021. See the published version at https://doi.org/10.1186/s12935-021-01851-w.

Abstract

BACKGROUND

Neuroblastoma is a childhood neural crest tumor showing large clinical and genetic heterogeneity, one form displaying 11q-deletion is very aggressive. It has been shown that 11q-deletion results in decreased expression of *DLG2*, a gene residing in the deleted region. *DLG2* has a number of different isoforms with the main difference is the presence or absence of a L27 domain. The L27 domain containing DLG proteins can form complexes with CASK/MPP and LIN7 protein family members, which will control cell polarity and signaling.

METHODS

We evaluated the DLG gene family and the LIN7 gene family for their expression in differently INSS staged neuroblastoma from publically available neuroblastoma data and primary tumors, we included two distinct *DLG1* and *DLG2* N-terminal transcript isoforms encoding L27 domains for their expression. Functionality of *DLG2* isoforms and of *LIN7A* were evaluated in the 11q-deleted neuroblastoma cell line SKNAS.

RESULTS

In neuroblastoma only two *DLG2* isoforms were expressed: isoform 2 and isoform 7/8. Using the array data we could determine that higher expression of DLG members that contain L27 domains correlated to better survival and prognosis. Whilst *DLG1* showed a decrease in both isoforms with increased INSS stage, only the full length L27 containing *DLG2* transcripts *DLG2-isoform 7/8* showed a decrease in expression in high stage neuroblastoma. We could show that the protein encoded by *DLG2-isoform 7* could bind to LIN7A, and increased *DLG2-isoform 7* gene expression increased the expression of *LIN7A*, this reduced neuroblastoma cell proliferation and viability.

CONCLUSION

We have provided evidence that gene expression of the L27 domain containing *DLG2-isoform 7/8* but not L27 domain lacking *DLG2-isoform 2* is disrupted in neuroblastoma, in particular in the aggressive subsets of tumors. The presence of the complete L27 domain allows for the binding to *LIN7A,* which will control cell polarity and signaling, thus affecting cancer cell viability.

Background

Neuroblastoma is a pediatric tumor arising from the transient embryonic neural crest, with tumor formation in the sympathetic division of the autonomous nervous system, it is one of the most common forms of extra cranial solid tumors found in young children (1). The clinical diagnosis of neuroblastoma is difficult in part due to the age of the patient and the vague and indirect initial appearance of the symptoms (2). Neuroblastoma is post surgically staged according to the International Neuroblastoma Staging System (INSS). INSS stages 1 and 2 are complete or partially resected localized tumors, stage 3 denotes the larger localized tumors that cross the midline. Stage 4 tumors have dissemination of the tumor to lymph nodes or bone marrow and often has poor survival. Stage 4 s are special cases, where the patient is younger than one year old, with a one sided tumor with metastasis to the liver or skin but less than 10% bone marrow involvement (3). The survival prognosis of the 4 s stage patients is lower than the stage 2 tumor group but better than the stage 3 tumor group (4). Within the higher staged tumors there are also subtypes with varying genetic alterations.

One of the common alterations that occur in neuroblastoma is deletion of a segment of chromosome 11 often 11q14-ter (5, 6). Within this deleted region resides the candidate tumor suppressor gene Discs Large Homologue 2 (*DLG2)*, and

lowered expression of *DLG2* is seen in advanced neuroblastomas with 11q-deletion or with *MYCN*-amplification (7), also ALK activity seems to affect the *DLG2* expression (8). Low *DLG2* level forces cell cycle progression (7) and maintain an undifferentiated state in neuroblastoma cells (8). Furthermore, abnormally low *DLG2* expression has been detected in the human cancers osteosarcoma (9) and ovarian cancers (10). The DLG family has significant functions governing polarity, cellular structure and growth behavior (11–13). These functions are thought to be achieved by protein trafficking to the cellular surface of epithelial cells as well as the organization and stabilization of supramolecular adhesion and signaling complexes through heterodimeric formation (14). Currently, five human homologs of the *DLG* family have been identified; *DLG1* (chromosomal location: 3q29) (encodes protein: SAP97), *DLG2* (11q14.1) (PSD93), *DLG3* (Xq13.1) (SAP102), *DLG4* (17p13.1) (PSD95) and *DLG5* (10q22.3) (disks large homologue 5). The DLG family are required to have; 3 PDZ domains, a SH3 domain and a guanylate kinase (GUK) domain.

DLG1, DLG2 and *DLG4* have various transcription isoforms that either contain or lack a L27 domain. For the DLG family, the proteins that lack the L27 domain are designated as the α-protein and contain N-terminal palmitoylated cysteines, derived from two codons that are mutually exclusive to the β-protein (15). The variants that contain the L27 domain are designated as the β-protein with the exception of *DLG2* (Fig. 1a). *DLG1* and *DLG4* have 2 exons encoding the L27 domain whereas *DLG2* (PSD93) has 5 exons encoding the L27 region and SH3 linker region. The currently accepted PSD93β protein is *DLG2* isoform 1 which does not include exon 1 or the start of exon 2 and thus follows the standard exon structure of *DLG1* and *DLG4*. This discrepancy was highlighted by Parker *et. al.* in 2004 (16), where they showed that isoforms 7 and 8 (PSD-93ζ) is the full length protein containing the first three exons resulting in a complete L27 domain and the 2 associated with the linker domain. It has even been suggested that it should be renamed as PSD93β (17). The difference between isoforms 7 and 8 is a single codon with isoform 7 the longer of the two. *DLG2* Isoform 2 (PSD93α), has no L27 domain and has a separate initiation site at exon 6 encoding the palmitoylated cysteines (Fig. 1b). *DLG4* has been shown to have transcripts either with or without a L27 domain (15). The DLG family transcripts with the complete L27 domain have been shown to be able to form L27 mediated tripartite complexes (18). Alternatively, the isoforms lacking the L27 domains have shown to have palmitoylated cysteines that target to the synapses (15) and increase synaptic strength (15, 19, 20). The remaining two members of the DLG family, *DLG3* and *DLG5* completely lack the L27 domain and N-terminal cysteines in all isoforms (Fig. 1a). *DLG3* (SAP102) is regulated by the SH3 and GUK domain and is often found in immature neurons, suggesting a specific role in neuron growth and development (21). Overexpression of *DLG3* has been previously shown to both result in a loss of adhesion properties in esophageal cells (22) and decreased survival in breast cancer (23). *DLG5* has been shown to be lost in breast cancer (24) with restoration of *DLG5* expression inhibiting cell migration and proliferation (25).

The L27 domain is a supramolecular assembly domain that is found in receptor targeting proteins such as CASK and LIN7 which results in the formation of a tripartite complex (26, 27). The Lin7 family consists of three members, Lin7a (26 kD), Lin7b (23 kD), and Lin7c (22 kD), each of which has an L27 domain and a PDZ domain. The L27 domain is most closely associated with the assembly of signaling complexes and cell polarity complexes (28) by localizing to tight junctions (27), important for cell architecture and growth signaling in all cells, including cancer cells. The interaction, which is also found in *Drosophila melanogaster*, is often a tripartite interaction with three proteins forming complex of four L27 domains (27, 29). For the tripartite protein complex to form, a protein with two L27 domains like the MPP or CASK families are first required (30). Subsequently the second L27 domain is provided by the Lin7 family with the final L27 domain been provided by the DLG family (31). The L27 domain has been shown to direct protein binding so that the resulting complex is diverse and does not contain homodimerization (31), which is otherwise common within the broader MAGUK superfamily of which the DLG family are members.

In this study we have considered the expression of all DLGs, especially considering the L27-domain containing DLG-isoforms, and the important L27-containing interaction partner LIN7A in neuroblastoma. We have evaluated the different

isoforms of *DLG2*, affected by the common 11q-deletion and *MYCN*-amplification in advanced staged neuroblastoma, and how they relate to the tripartite complex.

Methods

Gene expression analysis

Data for analyses and comparison of *DLG2* expression between the different patient subgroups for was imported from the R2 platform (http://r2.amc.nl). The independent neuroblastoma primary datasets; 1): SEQC GSE49710 (microarray), 2): Neuroblastoma NCI TARGET data (RNA-seq) for gene expression and transcript expression. The results generated from the NCI TARGET data was generated by the Therapeutically Applicable Research to Generate Effective Treatments (https://ocg.cancer.gov/programs/target) initiative, phs000218. The data used for this analysis are available at https://portal.gdc.cancer.gov/projects. RNA from SKNAS cells and from 22 fresh frozen primary neuroblastoma samples; 5 stage 1–2, 9 stage 3 and 8 stage 4 tumors; were extracted using RNeasy Kit® (Qiagen) according to manufacturer's protocol. RNA was quantified by NanoDrop (NanoDrop Technologies) and 2 µg of RNA was reverse-transcribed into double stranded cDNA on a T-professional Basic Gradient thermal cycler (Biometra) using the High Capacity cDNA Reverse Transcription kit (Applied Biosystems). cDNA corresponding to 20 ng of RNA was used for each qPCR reaction. Transcript sequences of the isoforms of *DLG2* were obtained by FASTA search with the human cDNA sequence for each gene. Reactions were prepared for each cDNA using the SYBR® Green Master Mix protocol (Applied Biosystems), primers used according to Table 1.

Table 1
DLG2 NCBI reference sequence and PCR primer target sequence

NCBI Reference Sequence	Isoform	Protein	Forward Primer (5' to 3')	Reverse Primer (5' to 3')
NM_001142699.1	Isoform 1, 7 and 8	PSD93β (975aa)	GCACGGAGCAAGAAGGGAT	AGCTTATTCCAAGCTTTGCT
NM_001364.3	Isoform 2	PSD93α (870aa)	GCTCTCACTCAGTGCCTTCA	GTCCGGAGTGCACAGTAACA
NM_001142700.2	Isoform 3	PSD93 (749aa)	TTTGAGTGTTACCAGCTTTCGCT	TTTCTGTCCCATTGACCGGA
NM_001142702.2	Isoform 4	PSD93 (334aa)	TCAGGTTCCGCTAGTGAGTT	AACCGTCGTCACCTAATCCG
NM_001351274.2 NM_001351275.2	Isoform 7 Isoform 8	PSD93ζ (969aa/968aa)	AGAAGACAGATACTGACCGAGC	CACGGAGCAAGAAGGGATGT

Ethics statement

Primary neuroblastoma samples were collected for which written or verbal consent was obtained according to the ethical permits approved by the Karolinska University Hospital Research Ethics Committee (approval no 2009/1369-31/1 and 03-763).

Cell Lines and Cell culture

Human neuroblastoma cell line SKNAS and HEK293 were obtained from ATCC Cell Line Collection. The cell lines were maintained in RPMI 1640 supplemented with 10% FBS, 1% L-Glutamine, 1% HEPES solution and 1% sodium pyruvate.

Cells were maintained at 37 °C with 5% CO_2.

Plasmids, siRNAs and transfections

DLG2 (NM_001364) and DLG2 (NM_001351274.2) overexpression plasmids on a backbone of pcDNA3.1/C-(K)-DYK (OHu25658D and OHuq102626D respectively) vector were purchased from GenScript. LIN7A (NM_004664) over expression plasmid on a backbone of pCMV6-AC-GFP (PS100010) was purchased from Origene (RG221902). siRNA targeting *DLG2* (s4122), *LIN7A* (s16836) or Silencer™ Select Negative control No. 1 siRNA (4390843) was purchased from Ambion (ThermoFischer Scientific). SKNAS and HEK293 cells were grown to 80% confluence and subsequently transfected with; DYK-tagged *DLG2 isoform 7*, DYK-tagged *DLG2 isoform 2*, combined with GFP-tagged *LIN7A*, empty vector "mock" (pCMV6-AC-GFP), si-*LIN7A* or scrambled negative control "mock". 100 ng of DNA or 10 pmol siRNA was complexed with 0.3 µl of Lipofectamine 2000 according to the Lipofectamine 2000 reagent forward transfection protocol (Invitrogen; Thermo Fisher Scientific, Inc.).

Cell growth, proliferation and signaling

100 µl cell suspension of SKNAS (1×10^4 cells/well) was seeded in 96-well culture plates (Corning Incorporated). After culturing to 80% confluence the supernatant was removed and transfection media was added to the cells. 48 hours post transfection, cells were counted using a 60 µm sensor for the Scepter handheld cell counter (Millipore) as per the manufactures instructions (32). Cell proliferation was measured using the MTS/MPS Cell Titer 96® One solution Reagent (Promega) and detecting the color variation (FLUOstar Omega, BMG Labtech) as per the manufacturer's recommendations. The absorbance values were normalized to the mock transfection and expressed as a percentage. All experiments were repeated three times.

Protein Co-immunoprecipitation and Western blot

Protein was extracted from the transfected cells in 6 well plates (1×10^5 cells/well), by aspirating the media and incubating on ice for 5 minutes then adding ice cold mPER buffer (Thermo-fisher Scientific, 78505). The lysate was then co-immunoprecipitated using µMACS isolation kits for DYKDDDDK (Miltenyi Biotech, 130-101-591) and for GFP (Miltenyi Biotech, 130-091-288). Western blot analysis was performed using a Mini-PROTEAN® TGX™ 8–20% gradient gel (Bio-Rad), protein was blotted onto LF-PVDF membrane (8 minutes, 25V and 2.5A) using a Trans-Blot® Turbo™ Transfer System (Bio-Rad). Blots were subsequently blocked for 1 hour in 5% milk in TBST buffer (0.1% Tween-20 and 150 mM NaCl in 10 mM Tris–HCL, pH 7.4) as per the manufacturer's recommendations. Blots were probed overnight at 4 degrees with antibodies diluted in PBST (0.1% Tween-20 in PBS). Primary antibodies; FLAG tag (FG4R, 1:1000, Invitrogen) and LIN7A (PA5-30871, 1:1000, Invitrogen). All primary antibodies were diluted to 1:1000 in PBST 0.1%. The secondary antibodies used for detection were; Starbright goat anti-Rabbit 1:2500 (12004161, Biorad) and Alexa 488 goat anti mouse 1:5000 (A28175). All wash stages were 3 × 10 minutes in TBST 0.1%. Secondary antibodies were incubated for 1 hour at room temperature. Image detection was performed on ChemiDoc MP (Biorad).

Statistical analysis

All data presented are plotted as Tukeys box and whisker plots showing IQR, line at the median, + at the mean with whiskers ± 1.5-fold of interquartile range from at least 3 independent experiments. For all multi-group analyses, differences were determined by one way ANOVA test followed by Holm-Sidak's multiple comparison test. For comparisons between two groups a Mann-Whitney *U* test was used: $^{*}p < 0.05$, $^{**}p < 0.01$, $^{***}p < 0.001$. All analyses were conducted using GraphPad Prism version 8.4.3 for Windows, (GraphPad Software, www.graphpad.com).

Results

Expression of DLG members with L27 domains were inversely correlated to survival and risk

The main difference between different proteins encoded by DLG gene members and their isoforms is the presence or absence of an N-terminal L27 domain (Fig. 1a). The exon structure of *DLG2* showing the initiation sites of the ζ, β, α, ε, δ and γ isoforms (Fig. 1b) (16, 17). We evaluated the association of DLG family expression with survival and risk, using online microarray data using the neuroblastoma patient dataset (GSE49710) obtained from the R2 Genomics Analysis and Visualization Platform (http://r2.amc.nl). The data was divided into survival outcome; alive or deceased (Fig. 1c). The L27-containing DLG members *DLG1* (log2 fc = 0.30, $p < 0.001$), *DLG2* (log2 fc = 0.72, $p < 0.001$) and *DLG4* (log2 fc = 0.49, $p < 0.001$) all showed higher expression in surviving cases, whereas the non-L27-containing *DLG3* (log2 fc =-0.23, $p < 0.001$) showed lower expression, *DLG5* showed no difference in expression (Fig. 1c). The same trend was seen for risk stratification with *DLG1* (log2 fc = 0.40, $p < 0.001$), *DLG2* (log2 fc = 0.68, $p < 0.001$) and *DLG4* (log2 fc = 0.72, $p < 0.001$), all showed higher expression in low risk neuroblastoma whereas *DLG3* (log2 fc =-0.47, $p < 0.001$) showed lower expression in low risk neuroblastoma (Fig. 1d).

We evaluated the expression levels in neuroblastoma of the L27-domain containing DLG family members, *DLG1*, *DLG2* and *DLG4*, by comparing the total gene expression and transcript encoding the alpha or beta protein using the using online data using the neuroblastoma patient dataset (TARGET) obtained from the R2 Genomics Analysis and Visualization Platform (http://r2.amc.nl). The data was divided into INSS stage for *DLG1*, *DLG2* and *DLG4*. *DLG1* showed a decrease in *DLG1* isoform 1 (*DLG1-iso1)* (ENST00000452595) expression corresponding to SAP-97α between stage 4 and the favorable stage 4 s (log2 FC = 0.44, $p < 0.001$) with no difference between stage 3 and 4 (Fig. 2a). *DLG1* showed a decrease in *DLG1* isoform 2 (*DLG1-iso2)* (ENST00000357674) transcript expression corresponding to L27-containing SAP-97β, between stage 4 and stage 4 s (log2 FC = 0.44, $p < 0.001$) and between stage 3 and stage 4 s (log2 FC = 0.76, $p < 0.05$) (Fig. 2a). At the total gene expression level a similar decrease in expression as the *DLG1-iso2* transcript was observed between stage 4 and stage 4 s (log2 FC = 0.80, $p < 0.001$) and between stage 3 and stage 4 s (log2 FC = 0.76, $p < 0.05$) (Fig. 2a). *DLG2* showed no decrease in transcript *DLG2* isoform 1 (*DLG2-iso1)* (ENST00000376104) transcript expression corresponding to the truncated L27-containing SAP-93β or *DLG2* isoform 2 (*DLG2-iso2)* (ENST00000398309) expression, corresponding to non-L27-containing PSD-93α, between the stages. At the total gene expression level (including all *DLG2* isoforms) a decrease in expression is observed between stage 4 and stage 4 s (log2 FC = 0.72, $p < 0.001$) (Fig. 2b). Indicting that isoforms accounting for this difference have not been included in this analysis. *DLG4* showed no decrease in isoform 1 expression between the stages. Furthermore, there was no change in total *DLG4* expression level between stages (Fig. 2c).

DLG2 isoform 7/8 was downregulated in high stage neuroblastoma

We evaluated the expression of the main *DLG2* isoforms, using the transcript data from the TARGET dataset based off GRCh37. We determined that the *DLG2* isoforms with the highest expression were *DLG2-iso2* (ENST00000398309) and *DLG2* L27 only (ENST00000472545), with no or very low expression of isoforms 1 (ENST00000376104), 3 (ENST00000418306) or 4 (ENST00000280241) detected (Fig. 2d). In this chromosome build *DLG2-iso7* or 8 are not included and therefore cannot be included in the analysis. The presence of *DLG2* L27 only (ENST00000472545) indicates that isoforms 7/8 are likely expressed, but not captured in this expression data using this chromosome build. Using 22 primary neuroblastoma samples, we could confirm by qPCR the unaltered *DLG2*-iso2 expression observed in the TARGET dataset (Fig. 2e). We could also confirm that there was no expression of isoforms 3 or 4 in our samples. Isoform 1 as a truncated variant of isoforms 7 and 8 (Fig. 1b), cannot be uniquely identified by qPCR when compared to isoforms 7/8, and since the isoform 1/7/8 qPCR result showed the same result as the specific isoform 7/8 qPCR, we concluded that isoform 1 was not expressed in our samples (data not shown). No variation in the expression of *DLG2-iso2* (ENST00000398309) was observed between the stages (Fig. 2e), consistent with Fig. 2b. The *DLG2-iso7/8*

(ENST00000650630) transcript had decreased expression in the stage 4 tumors when compared to the stage 1 and 2 tumors (log2 FC = 3.1, $p < 0.05$). *DLG2-iso7/8* was also decreased compared to *DLG2-iso2* in stage 4 (log2 FC = 4.9, $p < 0.001$) but not between stage 1 + 2 and stage 3 tumors (Fig. 2e). To evaluate the total DLG expression in neuroblastoma we determined the relative expression in Fragments Per Kilobase Million (FPKM) of all DLG family members. *DLG1, DLG2* and *DLG3* all showed similar expression levels with *DLG4* and *DLG5* having significantly higher expression (Fig. 2f).

DLG2 expression correlated to *LIN7* family gene expression and neuroblastoma samples formed clusters.

The L27-domain enables binding to other L27-domain containing proteins. An important L27-containing scaffolding protein in signaling complex formation is the LIN7 protein family. The relationship between *DLG2* and *DLG1* and the various LIN7 binding partners was examined using primary tumor data taken from the Z score of 159 tumor data sets on the R2 Genomics Analysis and Visualization Platform (http://r2.amc.nl). A positive relationship ($Y = 0.82x - 0.05$, $P < 0.001$) between *DLG2* and *LIN7A* across tumor datasets could be confirmed (Fig. 3a). Clusters were formed based on the spatial coordinates of *DLG2* and *LIN7A* expression. Medulloblastoma (6/7), Ewings sarcoma (2/2), Glioma (6/7), Pheochromocytomas/Paragangliomas (2/2) and Neuroblastoma (5/5) all showed high *DLG2* expression as well as high *LIN7A* expression. The remaining tumors with similar expression included other tumors of the CNS such as Glioblastoma, Primitive neuroectodermal tumor (PNET) and other brain tumors. Squamous cell carcinoma (2/2) showed high *DLG2* expression with low *LIN7A* expression. The remainder of the tumor dataset consisting of Lung, Colon, Ovarian, Breast and various lymphomas tended to show low expression of both *DLG2* and *LIN7A* (Fig. 3a). A weak linear relationship could be established between *DLG1* and *LIN7A* (Fig. 3b), however no distinct tumor clusters could be formed. A positive relationship ($Y = 0.70x + 0.07$, $P < 0.0001$) could be established between *DLG2* and *LIN7B* across tumor datasets (Fig. 3c). Ewing's sarcoma (2/2) and Neuroblastoma (5/5) clustered with high *DLG2* expression as well as high *LIN7B* expression. No linear relationship ($Y = 0.66x + 0.08$, $P = 0.23$) between *DLG1* and *LIN7B* across tumor datasets could be confirmed (Fig. 3d). A positive relationship ($Y = 0.97x + 0.04$, $P < 0.0001$) between *DLG2* and *LIN7C* between tumor datasets could be confirmed (Fig. 3e). Ewings sarcoma (2/2) and Neuroblastoma (5/5) clustered with high *DLG2* expression as well as high *LIN7C* expression. Squamous cell carcinoma (2/2) clustered with high *DLG2* expression and low *LIN7C* expression (Fig. 3e). A positive relationship ($Y = 1.6x + 0.00$, $P < 0.05$) between *DLG1* and *LIN7C* across tumor datasets could be confirmed (Fig. 3d), however distinct tumor clusters were not formed.

DLG2-isoform 7 expression controlled *LIN7A* expression and the *DLG2-isoform 7* encoded protein can bind LIN7A

To further evaluate the relationship that was established in Fig. 3a between *DLG2* and *LIN7A* gene expression, we determined the expression of *LIN7A* and *DLG2-iso7/8* in neuroblastoma primary samples. A strong positive correlation ($R^2 = 0.89$, $Y = 1.1x - 0.06$, $P < 0.001$) between the expression of *DLG2-iso7/8* and *LIN7A* for 22 primary neuroblastoma tumors of varying stages was detected (Fig. 4a). To determine if the relationship was causal we over expressed *DLG2-iso7* or knocked down *DLG2* expression by siRNA treatment in SKNAS neuroblastoma cells. When *DLG2-iso7* was over expressed *LIN7A* expression increased, and *LIN7A* expression decreased following *DLG2* silencing (Fig. 4b). When *LIN7A* was over expressed or silenced by siRNA we saw no difference in total *DLG2* expression (Fig. 4c). To determine if *DLG2-iso7 or DLG2-iso2* bound directly to *LIN7A* we performed co-immunoprecipitation using co-transfected HEK-293 cells, showing that *DLG2-iso7* but not *DLG2-iso2* could bind to LIN7A (Fig. 4d).

LIN7A expression was low in high staged tumors and over expression changed the growth behavior of neuroblastoma cells.

To further investigate the importance of *LIN7A* we evaluated the association of LIN family expression with survival and INSS, using online microarray data in the neuroblastoma patient dataset (GSE49710) obtained from the R2 Genomics Analysis and Visualization Platform (http://r2.amc.nl). The data was divided into survival outcome; alive or deceased. *LIN7A* (log2 fc = 1.06, $p < 0.001$) showed a decrease in expression in the deceased patients compared to the patients that

survived (Fig. 5a). *LIN7B* (log2 fc = 0.43, p = 0.09) and *LIN7C* (log2 fc = 0.20, p = 0.66) showed no difference in expression (Fig. 5a). The expression of *LIN7A* was then stratified by INSS stage. Stage 4 tumors showed the lowest expression compared to stage 1 (log2 fc = 0.44, p < 0.01), stage 2 (log2 fc = 0.44, p < 0.001), stage 4 s (log2 fc = 0.25, p < 0.05) and stage 3 (log2 fc = 0.50, p < 0.01) (Fig. 5b). Over expression of *LIN7A* in neuroblastoma cells (SKNAS) resulted in slower proliferation compared to the control (Fig. 5c, p < 0.001). We observed a decrease in the number of viable cells (Fig. 5d, p < 0.001) and an increase in the non-viable cell fraction (Fig. 5d, p < 0.001) in cells with increased *LIN7A* expression. *LIN7A* silencing in SKNAS cells resulted in an increase in cell proliferation (Fig. 5c, p < 0.01), with an associated increase in viable cell number, no effect in the non-viable cell number was observed (Fig. 5d). The *LIN7A* over expression after expression plasmid transfection, and *LIN7A* silencing by siRNA treatment of neuroblastoma cells (SKNAS) was confirmed by qPCR (Fig. 5e).

Discussion

We have previously established that *DLG2* is a candidate tumor suppressor gene with importance in 11q deleted neuroblastoma as well as a downregulated target of *MYCN* amplification in neuroblastoma (7). During which, we did not explore the various isoforms of *DLG2* and the effects that the resulting proteins have on neuroblastoma. As we have shown in Fig. 1a *DLG1*, *DLG2* and *DLG4* all have isoforms that either contain an N-terminal L27 domain or palmitoylated cysteines. When the palmitoylated cysteines are present they modulate homo- or heterodimers with other palmitoylated cysteines that bind synaptic proteins, contributing to the function and strength of the post synaptic density (33). We could show that there was an overall loss of *DLG1* in the high INSS stage tumors with no difference seen between the α- and β-isoforms (Fig. 1b and 2a). We could also show that *DLG4* isoform expression was not altered in any of the neuroblastoma stages (Fig. 2c) despite showing that higher expression correlated with both survival and prognosis (Fig. 1c and d). We showed that *DLG2* displayed differential isoform expression in the high INSS tumors (Fig. 2e). The decreased expression of the L27 domain containing *DLG2 isoform 7/8* in the high stage neuroblastoma (Fig. 2e) highlights the importance of the L27 domain of *DLG2* in neuroblastoma.

The L27 domain is involved in protein interactions, mainly the formation and correct localization of scaffolding and receptor proteins. The localization of L27 domain containing proteins to the membrane bound receptors indicates a signaling regulatory role in these receptors. The formation of the tripartite complexes is known to contain four L27 domains (30), with one protein such as CASK or the MPP family providing two L27 domains and serving as the platform on which the complex is built (30). The L27 domain containing members of the DLG family have been shown to bind to the N-terminal L27 domain, whereas the LIN family has been shown to bind to the adjacent L27 domain (30). The presence of the L27 domain is important for the binding of *DLG2* encoding proteins into this complex. The LIN7 that is present also determines which DLG will likely bind, with *DLG1* encoding proteins and LIN7C showing a strong preference, replicating the already known binding patterns (27, 34). Whereas, *DLG2* is more of a generalist with expression correlating to all LIN7 homologues (Fig. 3a, c and e), however the clear stratification of tumors seen with *DLG2* and *LIN7A* indicates there may be a causal relationship between the two (Fig. 3a). We were able to show that an increase in *DLG2-iso7* resulted in an increase in *LIN7A* expression (Fig. 4b), but there was no alteration in total *DLG2* expression when *LIN7A* was over expressed (Fig. 4c). Furthermore we could show that *DLG2-iso2* cannot bind to LIN7A showing that the L27 domain of *DLG2-iso7* is required for this binding to occur (Fig. 4d). The binding complexes that form as a result of the different L27 containing DLG members will likely have slight functional differences, depending on which base protein is present as well as which DLG and LIN7 family members are bound into the complex, yet have a high degree of redundancy (35). The various permutations of the base protein, DLG and LIN7 families exponentially expand the different types of the complex that can form.

The depletion of *LIN7A* in neurons has previously been shown to result in abnormal neuronal migration (36), a feature of neuroblastoma (37). Clinical cases have also shown that loss of the *LIN7A* loci results in cellular hyperplasia (36). We

were able to replicate these clinical results with the knockdown of *LIN7A* in neuroblastoma cells, resulting in increased cell number and proliferation (Fig. 5c-d). However, increased *LIN7A* expression has been previously shown to be associated with a loss of polarity in breast cancer cells (38) as well as increased proliferation in hepatocellular carcinoma (39) and ovarian cancer (40). Our analysis showed that these previously established tumor types in which *LIN7A* is oncogenic or disruptive tended to cluster with low *DLG2* expression in Fig. 3a. Tissue specificity may account for the altered function observed.

The deletion of 11q in neuroblastoma is known to be heterozygous and hence leaves one copy of any potential tumor suppressor gene in this region. It has been established that any TSG will probably be involved in a haploinsufficient mechanism due to the general lack of a second hit. Having a gene with two distinct structural isoforms with separate functions resulting in differing protein localization increases the likelihood that *DLG2* may have a haploinsuffient mechanism. The fact that the other members of the DLG family with L27 domains have such a high degree of structural homology, the correct function of the tripartite complex as a whole must be important to the cell. We suggest that whilst there is probably a high degree of redundancy within the DLG family for the tripartite complex function it is most likely highly sensitive to disruptions like 11q deletion or lower expression of another DLG family member.

Conclusions

We have provided evidence that gene expression of the L27 domain containing *DLG2-isoform 7/8* but not L27 domain lacking *DLG2-isoform 2* is disrupted in neuroblastoma, in particular in the aggressive subsets of tumors. The presence of the complete L27 domain allows for the binding to *LIN7A*, which will control cell polarity and signaling, thus affecting cancer cell viability.

Abbreviations

International Neuroblastoma Staging System (INSS), Discs Large Homologue 2 (*DLG2)*, guanylate kinase (GUK), isoform (*iso)*

Declarations

Ethics approval and consent to participate

Primary neuroblastoma samples were collected for which written or verbal consent was obtained according to the ethical permits approved by the Karolinska University Hospital Research Ethics Committee (approval no 2009/1369-31/1 and 03-763).

Consent for publication

All authors give consent for the publication of the manuscript.

Availability of data and materials

The datasets analyzed during the current study are available in the 'R2: Genomics Analysis and Visualization Platform repository, [http://r2.amc.nl]. The datasets analyzed are SEQC GSE49710 (microarray) and Neuroblastoma NCI TARGET data (RNA-Seq). The results generated from the NCI TARGET data was generated by the Therapeutically Applicable Research to Generate Effective Treatments (https://ocg.cancer.gov/programs/target) initiative, phs000218. The data used for this analysis are available at https://portal.gdc.cancer.gov/projects

Competing interests

The authors declare that they have no competing interests.

Funding

This work was supported by grants from the Swedish Childhood Cancer Fund, Jane and Dan Olsson Foundation and Assar Gabrielsson Fund. The funders were not involved in study design, data collection and analysis, decision to publish, or preparation of the manuscript.

Authors' contributions

KE generated conception and designed this study and provided technical and material support. SK developed the methodology, performed the assays, analyzed and interpreted the data. TM and PK provided clinical and genetic data and samples. SK and KE organized the data and wrote the manuscript. All authors read and approved the final manuscript.

Acknowledgements

We thank the Swedish Childhood Cancer Fund, Jane and Dan Olsson foundation, Assar Gabrielssons Foundation and University of Skövde for financial support.

References

1. Pugh TJ. The genetic landscape of high-risk neuroblastoma. Nature Genetics. 2013(3):279.
2. Parmar R, Wadia F, Yassa R, Zenios M. Neuroblastoma: a rare cause of a limping child. How to avoid a delayed diagnosis? Journal Of Pediatric Orthopedics. 2013;33(4):e45–51.
3. Smith EI, Haase GM, Seeger RC, Brodeur GM. A surgical perspective on the current staging in neuroblastoma–the International Neuroblastoma Staging System proposal. J Pediatr Surg. 1989;24(4):386–90.
4. Shuangshoti S, Shuangshoti S, Nuchprayoon I, Kanjanapongkul S, Marrano P, Irwin MS, et al. Natural course of low risk neuroblastoma. Pediatr Blood Cancer. 2012;58(5):690–4.
5. Caren H, Kryh H, Nethander M, Sjoberg R-M, Trager C, Nilsson S, et al. High-risk neuroblastoma tumors with 11q-deletion display a poor prognostic, chromosome instability phenotype with later onset. Proceedings of the National Academy of Sciences of the United States. 2010(9):4323.
6. Mlakar V, Jurkovic Mlakar S, Lopez G, Maris JM, Ansari M, Gumy-Pause F. 11q deletion in neuroblastoma: a review of biological and clinical implications. Mol Cancer. 2017;16(1):114.
7. Keane S, Ameen S, Lindlof A, Ejeskar K. Low DLG2 gene expression, a link between 11q-deleted and MYCN-amplified neuroblastoma, causes forced cell cycle progression, and predicts poor patient survival. Cell Commun Signal. 2020;18(1):65.
8. Siaw J, Javanmardi N, Van den Eynden J, Lind D, Fransson S, Marinez-Monleon A, et al. 11q Deletion or ALK Activity Curbs DLG2 Expression to Maintain an Undifferentiated State in Neuroblastoma. Cell Reports. 2020; in press.
9. Shao YW, Wood GA, Lu J, Tang QL, Liu J, Molyneux S, et al. Cross-species genomics identifies DLG2 as a tumor suppressor in osteosarcoma. Oncogene. 2019;38(2):291–8.

10. Zhuang RJ, Bai XX, Liu W. MicroRNA-23a depletion promotes apoptosis of ovarian cancer stem cell and inhibits cell migration by targeting DLG2. Cancer Biol Ther. 2019:1–15.
11. Roberts S, Delury C, Marsh E. The PDZ protein discs-large (DLG): the ' Jekyll and Hyde' of the epithelial polarity proteins. FEBS J. 2012;279(19):3549–58.
12. Ludford-Menting MJ, Thomas SJ, Crimeen B, Harris LJ, Loveland BE, Bills M, et al. A functional interaction between CD46 and DLG4: a role for DLG4 in epithelial polarization. The Journal Of Biological Chemistry. 2002;277(6):4477–84.
13. Liu J, Li J, Ren Y, Liu P. DLG5 in cell polarity maintenance and cancer development. International Journal Of Biological Sciences. 2014;10(5):543–9.
14. Papagiannouli F, Mechler BM. Refining the role of Lgl, Dlg and Scrib in Tumor Suppression and Beyond: Learning from the Old Time Classics. InTech, 2012-02-03.; 2012.
15. Schluter OM, Xu W, Malenka RC. Alternative N-terminal domains of PSD-95 and SAP97 govern activity-dependent regulation of synaptic AMPA receptor function. Neuron. 2006;51(1):99–111.
16. Parker MJ, Zhao S, Bredt DS, Sanes JR, Feng G. PSD93 regulates synaptic stability at neuronal cholinergic synapses. J Neurosci. 2004;24(2):378–88.
17. Kruger JM, Favaro PD, Liu M, Kitlinska A, Huang X, Raabe M, et al. Differential roles of postsynaptic density-93 isoforms in regulating synaptic transmission. J Neurosci. 2013;33(39):15504–17.
18. Jo K, Derin R, Li M, Bredt DS. Characterization of MALS/velis-1, -2, and – 3: a family of mammalian LIN-7 homologs enriched at brain synapses in association with the postsynaptic density-95 NMDA receptor postsynaptic complex. J Neurosci. 1999;19(11):4189–99.
19. Liu M, Lewis LD, Shi R, Brown EN, Xu W. Differential requirement for NMDAR activity in SAP97beta-mediated regulation of the number and strength of glutamatergic AMPAR-containing synapses. J Neurophysiol. 2014;111(3):648–58.
20. Cai C, Li H, Rivera C, Keinanen K. Interaction between SAP97 and PSD-95, two Maguk proteins involved in synaptic trafficking of AMPA receptors. J Biol Chem. 2006;281(7):4267–73.
21. Zheng CY, Petralia RS, Wang YX, Kachar B, Wenthold RJ. SAP102 is a highly mobile MAGUK in spines. J Neurosci. 2010;30(13):4757–66.
22. Hanada N, Makino K, Koga H, Morisaki T, Kuwahara H, Masuko N, et al. NE-dlg, a mammalian homolog of Drosophila dlg tumor suppressor, induces growth suppression and impairment of cell adhesion: possible involvement of down-regulation of beta-catenin by NE-dlg expression. Int J Cancer. 2000;86(4):480–8.
23. Liu J, Li P, Wang R, Li J, Zhang M, Song Z, et al. High expression of DLG3 is associated with decreased survival from breast cancer. Clin Exp Pharmacol Physiol. 2019;46(10):937–43.
24. Liu J, Li J, Li P, Wang Y, Liang Z, Jiang Y, et al. Loss of DLG5 promotes breast cancer malignancy by inhibiting the Hippo signaling pathway. Sci Rep. 2017;7:42125.
25. Liu J, Li J, Ren Y, Liu P. DLG5 in cell polarity maintenance and cancer development. Int J Biol Sci. 2014;10(5):543–9.
26. Lin EI, Jeyifous O, Green WN. CASK regulates SAP97 conformation and its interactions with AMPA and NMDA receptors. J Neurosci. 2013;33(29):12067–76.
27. Bohl J, Brimer N, Lyons C, Pol SBV. The stardust family protein MPP7 forms a tripartite complex with LIN7 and DLG1 that regulates the stability and localization of DLG1 to cell junctions. J Biol Chem. 2007;282(13):9392–400.
28. Li Y, Karnak D, Demeler B, Margolis B, Lavie A. Structural basis for L27 domain-mediated assembly of signaling and cell polarity complexes. EMBO J. 2004;23(14):2723–33.
29. Bachmann A, Kobler O, Kittel RJ, Wichmann C, Sierralta J, Sigrist SJ, et al. A perisynaptic menage a trois between Dlg, DLin-7, and Metro controls proper organization of Drosophila synaptic junctions. J Neurosci. 2010;30(17):5811–

24.
30. Yang X, Xie X, Chen L, Zhou H, Wang Z, Zhao W, et al. Structural basis for tandem L27 domain-mediated polymerization. FASEB J. 2010;24(12):4806–15.
31. Petrosky KY, Ou HD, Lohr F, Dotsch V, Lim WA. A general model for preferential hetero-oligomerization of LIN-2/7 domains: mechanism underlying directed assembly of supramolecular signaling complexes. J Biol Chem. 2005;280(46):38528–36.
32. Ongena K, Das C, Smith JL, Gil S, Johnston G. Determining cell number during cell culture using the Scepter cell counter. Journal of visualized experiments: JoVE. 2010(45):2204.
33. Waites CL, Specht CG, Hartel K, Leal-Ortiz S, Genoux D, Li D, et al. Synaptic SAP97 isoforms regulate AMPA receptor dynamics and access to presynaptic glutamate. J Neurosci. 2009;29(14):4332–45.
34. Lozovatsky L, Abayasekara N, Piawah S, Walther Z. CASK deletion in intestinal epithelia causes mislocalization of LIN7C and the DLG1/Scrib polarity complex without affecting cell polarity. Mol Biol Cell. 2009;20(21):4489–99.
35. Kamijo A, Saitoh Y, Sakamoto T, Kubota H, Yamauchi J, Terada N. Scaffold protein Lin7 family in membrane skeletal protein complex in mouse seminiferous tubules. Histochem Cell Biol. 2019;152(5):333–43.
36. Matsumoto A, Mizuno M, Hamada N, Nozaki Y, Jimbo EF, Momoi MY, et al. LIN7A depletion disrupts cerebral cortex development, contributing to intellectual disability in 12q21-deletion syndrome. PLoS One. 2014;9(3):e92695.
37. Johnsen JI, Dyberg C, Wickstrom M. Neuroblastoma-A Neural Crest Derived Embryonal Malignancy. Front Mol Neurosci. 2019;12:9.
38. Gruel N, Fuhrmann L, Lodillinsky C, Benhamo V, Mariani O, Cedenot A, et al. LIN7A is a major determinant of cell-polarity defects in breast carcinomas. Breast Cancer Res. 2016;18(1):23.
39. Luo CB, Yin D, Zhan H, Borjigin U, Li CJ, Zhou ZJ, et al. microRNA-501-3p suppresses metastasis and progression of hepatocellular carcinoma through targeting LIN7A. Cell Death Dis. 2018;9(5):535.
40. Hu X, Li Y, Kong D, Hu L, Liu D, Wu J. Long noncoding RNA CASC9 promotes LIN7A expression via miR-758-3p to facilitate the malignancy of ovarian cancer. J Cell Physiol. 2019;234(7):10800–8.

Figures

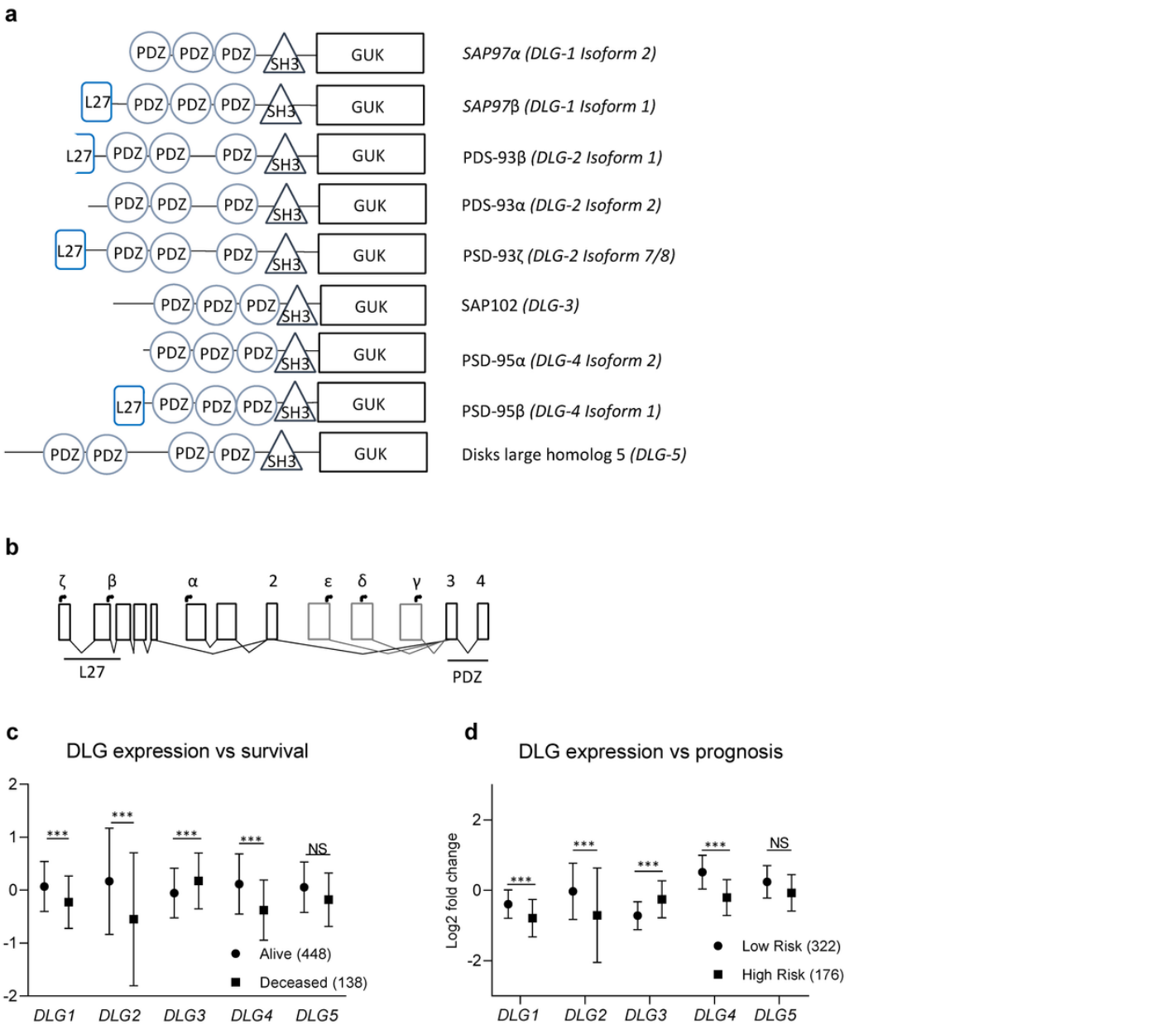

Figure 1

Domains found in DLG-encoded proteins, exon structure of DLG2 and DLG expression in neuroblastoma a The different isoforms of the DLG family with DLG1, DLG2 and DLG4 showing an isoform with L27 domain. The unique PSD93β protein, encoding just a partial L27 domain. The alpha isoforms of DLG1, DLG2 and DLG4 do not contain the L27 domains and thus have similar structures to DLG3. b The exon structure of DLG2 showing the 5 exons that make up the L27 and linker region in PSD93ζ with mutually exclusive initiation exons for PSD93α. Isoforms PSD93ε, PSD93δ and PSD93γ all have their initiation site after the common exon 2. Transcription start of DLG2 protein isoform indicated at the top, and protein domains at the bottom. Gene expression of the various DLG family members showing c survival and d prognosis for 586 patients from the online microarray data with the neuroblastoma patient dataset (GSE49710) obtained from the R2 Genomics Analysis and Visualization Platform (http://r2.amc.nl). The expression data are presented as centered log2 fold change and plotted as mean ±SD. *p < 0.05, **p < 0.01, ***p < 0.001.

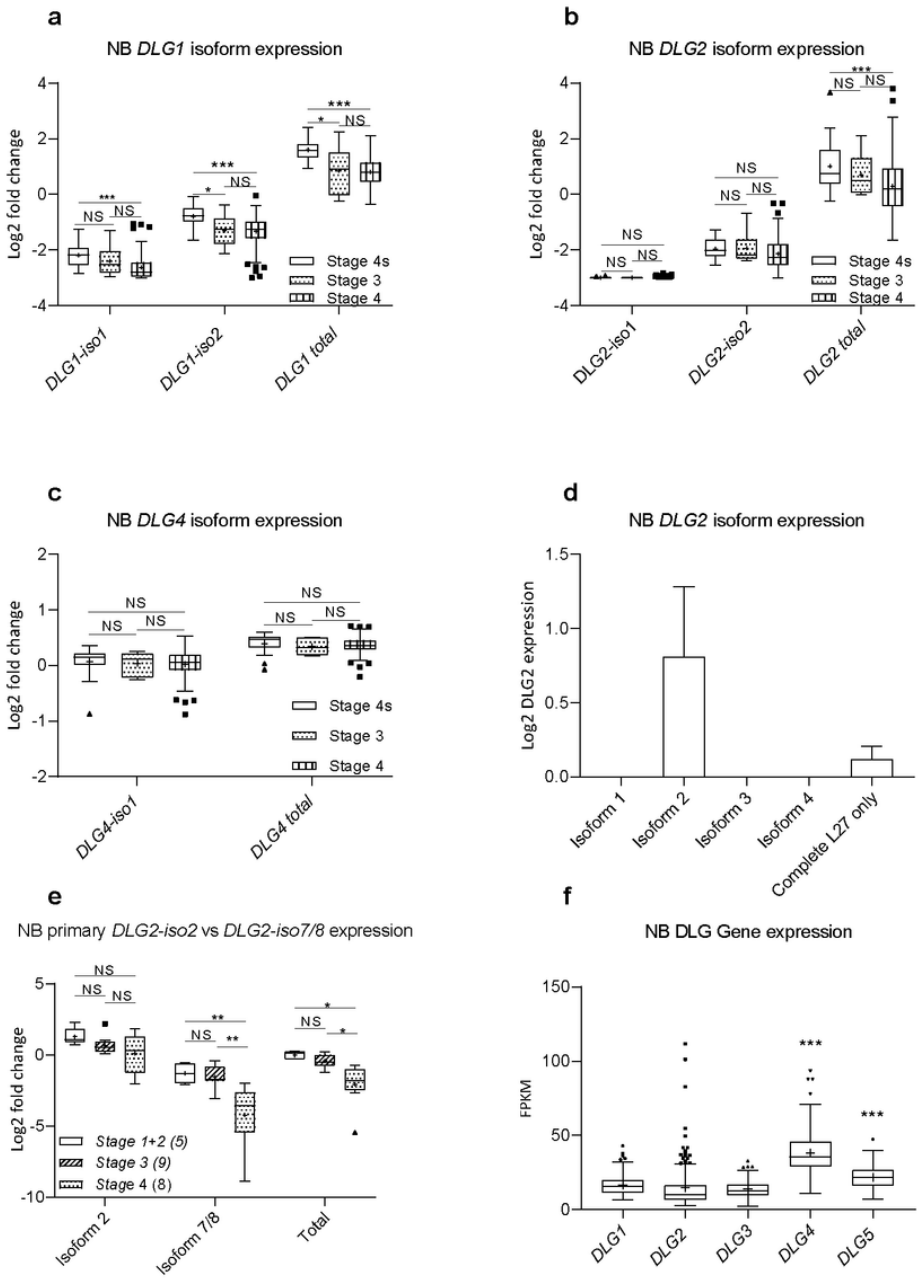

Figure 2

Comparison of DLG family member isoforms by stage DLG family isoform and total gene expression by stage from the NCI TARGET data (https://ocg.cancer.gov/programs/target); phs000218 for a DLG1, b DLG2 c DLG4 and d total mean expression level of DLG2 isoforms in all NB stages. e qPCR data comparing DLG2-isoform 2 and DLG2-isoform 7/8 expression in 22 primary neuroblastoma tumors. f comparison of the relative total DLG expression in the NCI TARGET neuroblastoma dataset. The expression data are presented as median centred log2 fold change and plotted as Tukeys box and whisker plots showing IQR, line at the median, + at the mean with whiskers ±1.5-fold of interquartile range. Data outside the whiskers are shown as outliers. *p < 0.05, **p < 0.01, ***p < 0.001.

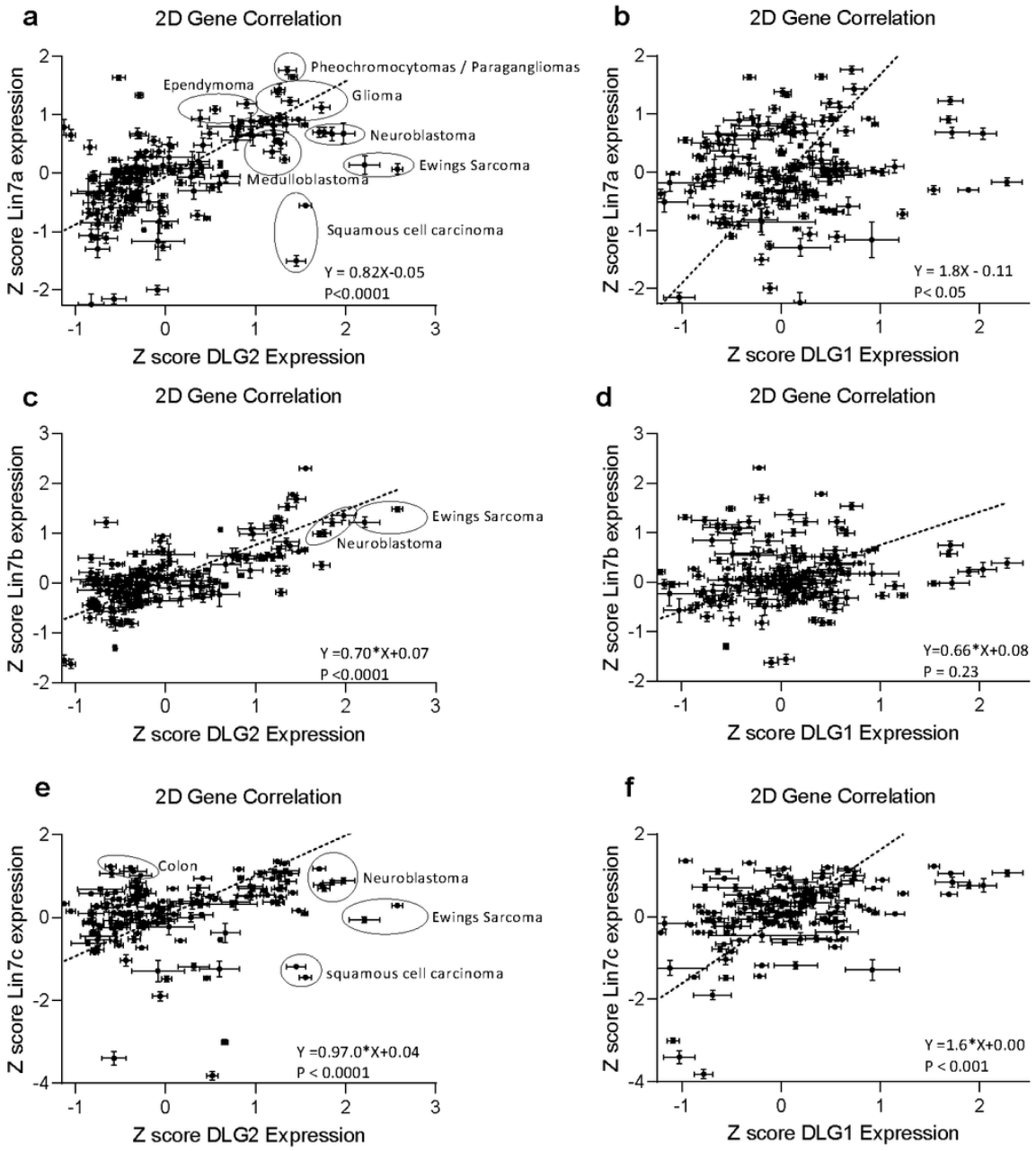

Figure 3

2D gene correlation of DLG1 and DLG2 with the LIN7 family across tumor datasets Scatter plots with data from 153 available differing tumor datasets sets on the R2 Genomics Analysis and Visualization Platform (http://r2.amc.nl), with LIN7 expression on the Y-axis and DLG expression on the X-axis using the gene expression mean Z score. a LIN7A and DLG2, b LIN7A and DLG1, c LIN7B and DLG2, d LIN7B and DLG1, e LIN7C and DLG2, f LIN7C and DLG1. The error bars are the standard deviation of the gene expression within the dataset. A line of best fit was created with a Deming (Model II) regression, the 95% confidence interval of the regression is also shown. Clusters were subsequently identified and highlighted.

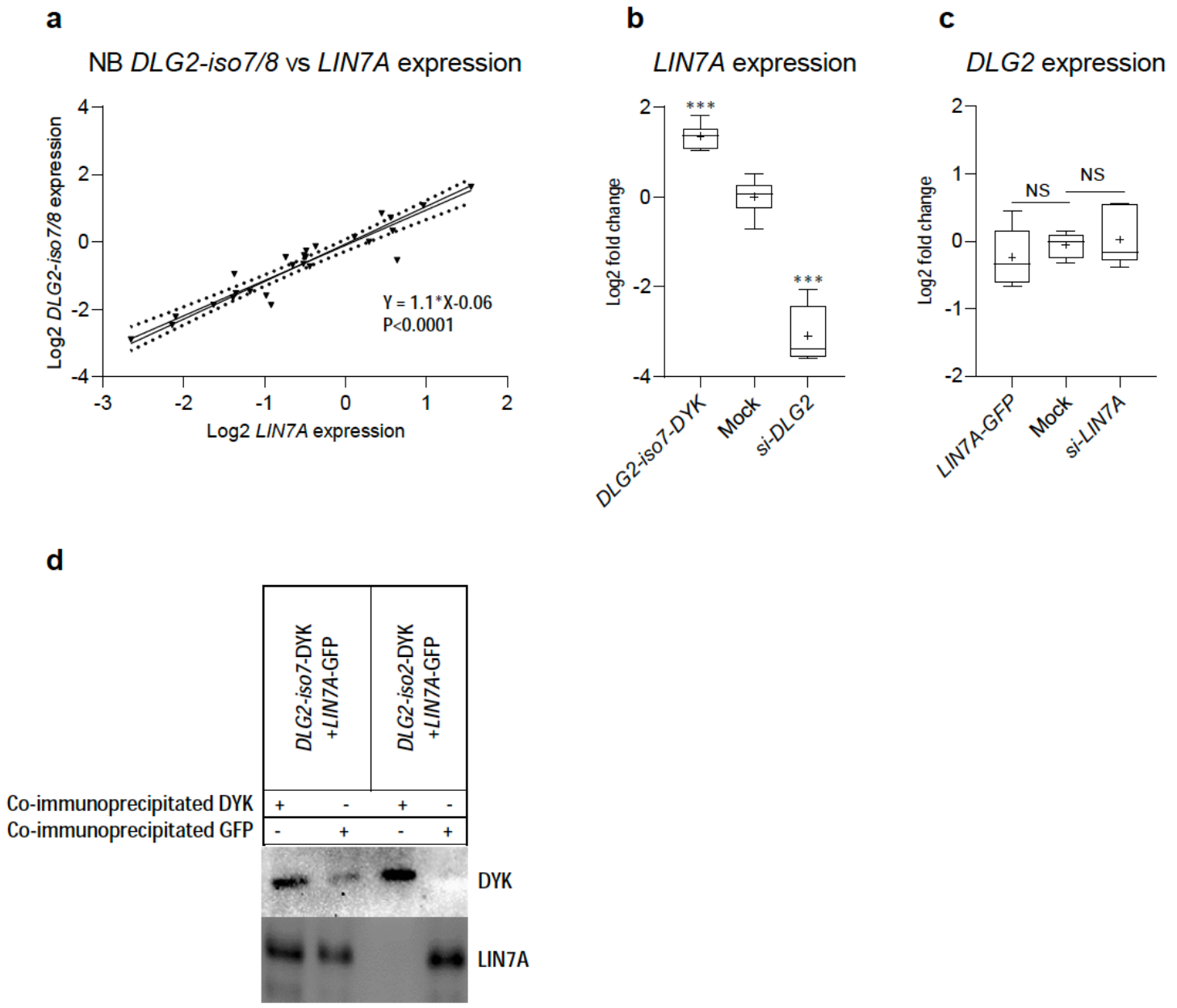

Figure 4

LIN7A expression is affected by DLG2-isoform 7 a The Relationship of DLG2-isoform 7/8 and LIN7A expression in 22 neuroblastoma primary tumor samples. The relative mRNA expression of DLG2 and LIN7A for each samples is determined. The data expressed as relative log2 fold change after normalization to GAPDH and GUSB with linearity determined using a line of best fit, created with a Deming (Model II) regression. b LIN7A gene expression 48 h post DLG2-isoform 7 over expression (DLG2-iso7-DYK) or silencing (si-DLG2) in SKNAS cells. c DLG2 gene expression 48 h post LIN7A over expression (LIN7A-GFP) or silencing (si-LIN7A) in SKNAS cells. d Co-immunoprecipitation of HEK293 cells co-transfected with DLG2-iso7-DYK and LIN7A-GFP or DLG2-iso2-DYK and LIN7A-GFP plasmids. Detection of the lysate with DYK or LIN7A antibody. ***p < 0.001

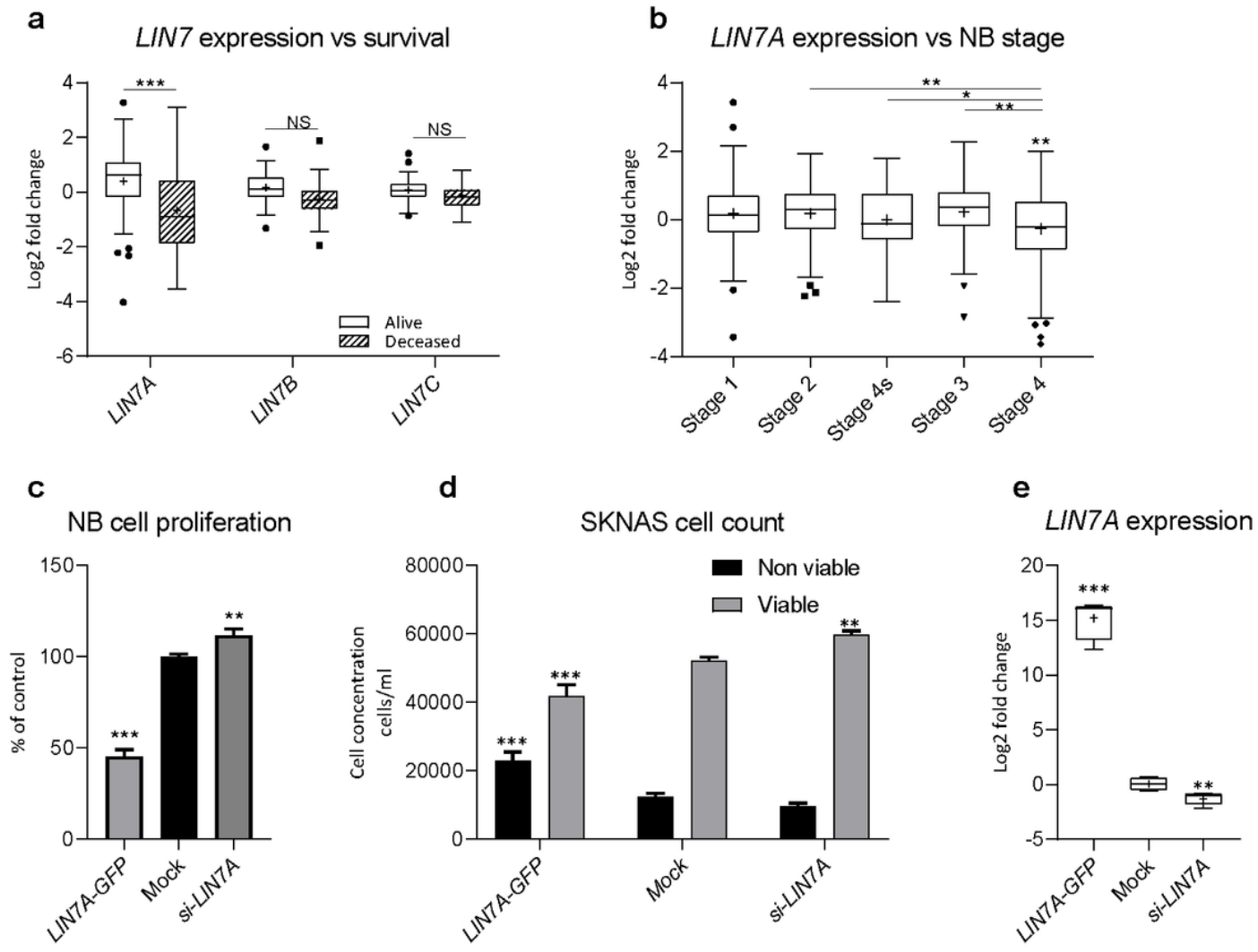

Figure 5

LIN7A expression in neuroblastoma correlates with survival and stage. LIN7 gene family expression in neuroblastoma patient dataset (GSE49710) stratified by a Survival b INSS stage. Cell responses 48 h post LIN7A over expression (LIN7A-GFP) or silencing (si-LIN7A) in SKNAS cells showing: c proliferation; d viable and non-viable cell fraction. e LIN7A gene expression analysis 48 h post LIN7A over expression (LIN7A-GFP) or silencing (si-LIN7A) in SKNAS. The data shown is the pooled average of 3 experiments. The data in c and d are shown as the mean ± SD. *p < 0.05, **p < 0.01, ***p < 0.001.